Stability of cross-linked acetic acid lignin-containing polyurethane

Haihua Wang · Yonghao Ni · M. Sarwar Jahan ·
Zehua Liu · Thioni Schafer

Abstract The thermo-oxidative stability of acetic acid lignin-containing polyurethane (LPU) that contains cross-linking agents, such as 1-aminopropyltriethoxy-silane (APTS) and/or trimethylolpropane (TMP) was investigated based on the thermogravimetric analysis (TGA) method, their kinetic parameters in the thermo-oxidative process was determined. FT-IR certified the occurrence of interaction between lignin and polyurethane (PU). It was found that continuous membrane can be formed when lignin concentration was 43.3%, but rupture took place when it increased to 50%. When the degradation was performed in nitrogen, TG and dynamic differential thermogravimetry (DTG) results demonstrated that the PU underwent three stages of degradation while the LPU involved one main degradation stage with a shoulder, and the degradation stability increased with the increase in the lignin concentration and PEG length. It was also found that the addition of a cross-linking agent is beneficial to the improvement of thermal stability and, in particular, APTS gave the best

thermal stability for the LPU produced, among the cross-linking agents tested. Furthermore, LPU exhibited multi-stage degradation process in air and displayed higher thermo-oxidative stability than PU. At the same time, the kinetic study showed that LPU modified with APTS exhibited higher activation energy than LPU modified with TMP. And the maximum activation energy was found for the sample modified with the simultaneous addition of APTS and TMP.

Keywords Acetic acid lignin · Polyurethane · Thermal degradation · Thermo-oxidative stability · Kinetics

Introduction

Lignin, as a nontoxic, low-cost, and renewable resource, has been considered as substitute for some petrochemical products to deal with petroleum resources crisis and environment pollution caused by non-biodegradable polymers [1, 2]. For instance, lignin as part of the starting material, has been studied to produce different polymers, such as polyurethane (PU) [3–5], phenol-formaldehyde resin [6, 7], polyester [8, 9]. It can also be used for blending with poly(ethylene oxide) [10], polyolefin [11, 12], polyester [13], and starch [14] and soy protein [15] to improve the strength, water resistance, thermal stability of the products. At present, the heat deformability/stability and compatibility with other components represent the major obstacles for the lignin-based polymer materials [2].

To minimize the use of chlorine- and sulfur-based chemicals in pulping and bleaching process, alternative pulping processes received much attention [16]. Organosolv methods are recognized as viable sulfur-free alternatives for traditional pulping techniques [17]. And lignin

H. Wang · Y. Ni · M. S. Jahan · Z. Liu · T. Schafer
Key Laboratory of Auxiliary Chemistry & Technology for
Chemical Industry, Ministry of Education. Shaanxi University
of Science & Technology, Xi'an Shaanxi 710021, China

H. Wang (✉) · Y. Ni · M. S. Jahan · Z. Liu · T. Schafer
Limerick Pulp and Paper Center, University of New Brunswick,
Fredericton, NB E3B 5A3, Canada
e-mail: hwang@unb.ca

H. Wang · Y. Ni · M. S. Jahan · Z. Liu · T. Schafer
Pulp and Paper Research Division, BCSIR Laboratories, Dhaka
Dhaka 1205, Bangladesh

H. Wang · Y. Ni · M. S. Jahan · Z. Liu · T. Schafer
Tianjin Key Laboratory of Pulp and Paper, Tianjin University
of Science and Technology, Tianjin 300457, China

produced from the so-called organic solvent pulping processes, is known to have better properties to be used as a potential raw material for polymers [18]. Mixture of ethanol/water [19, 20], in particular, a 60% ethanol solution [21], can be used to dissolve lignin in woody biomass, for example, mixed hardwood. Acetic acid and formic acid [22–24] are also effective organic solvents for lignin dissolution. In this investigation, we used acetic acid lignin (AL).

For PU, lignin and its derivatives can alternatively act as soft and hard-segment depending on its physical and chemical properties. To reduce the rigidity and brittleness, flexible diisocyanates and linear soft-segments such as polyethylene glycol (PEG) with different molecular weights were used [25, 26]. It was found that a low loading level of lignin could simultaneously enhance strength and elongation. However, a high lignin loading led to decrease in the toughness and other strength properties [27].

Chemical modifications such as esterification and etherification with alkylene oxides (especially ethylene oxide) have also been carried out on lignin to overcome the technical limitations and constraints imposed by lignin when directly used [5, 28]. The modified lignin can have similar functional characteristics (e.g. the hydroxyl group content) similar to conventional polyols used in PU synthesis. However, this type of modification increased the complexity of the process, thus, the production cost.

Cross-linking, from both physical and chemical mechanisms, can significantly affect the morphologies and properties of PU [29, 30]. The physical cross-linking may be due to the formation of hydrogen bonding and hard domain formation. The chemical cross-linking can be introduced into the system in many ways, such as using triol, higher functional polyol, having the isocyanate-to-hydroxy (NCO/OH) ratio greater than 1. In this paper, we studied to use cross-linking agents, including trimethylolpropane (TMP) and 1-aminopropyltriethoxy silane (APTS), in the synthesis of lignin-based polyurethane to enhance the properties of PU membranes, and therefore enlarge its application in plastics. TMP is a tri-functional alcohol and often used as self-cross-linking agent in the preparation of PU [31]. APTS has been utilized widely in many fields, such as the surface treatment, paints, coatings, and adhesives. And it is often employed to encapsulate silica in the preparation of hybrid PU nanocomposites [32, 33]. The use of a silane coupling agent for the preparation of lignin-based polyurethane (LPU) may be expected to provide improved thermal stability, elongation, and flexibility to the PU.

The objective of this work was to systematically evaluate the thermal behavior and thermo-oxidative stability of lignin-based polyurethane, and their kinetics. The thermal degradation of PU membranes is of great importance in

developing rational processing technologies and determining the end-user properties [34]. Furthermore, thermal properties are also a major factor to design bio-based material, which would have similar functions to those prepared from petroleum-based products [35].

Experimental

Reagent

The following reagents were used without further purification: methylene diphenyl diisocyanate (MDI), polyethylene glycol (PEG), 1-aminopropyltriethoxy-silane (APTS), trimethylolpropane (TMP), N, N-dimethylacetamide (DMAc); acetic acid, HCl, dioxane, diethyl ether, all of which were from Aldrich Chemicals; acetic acid lignin (AL) was prepared in our laboratory.

Preparation of acetic acid lignin (AL)

Spruce wood chips were submitted to a treatment with 90% acetic-acid solutions (500 mL) catalyzed by small amount (0.6%) of HCl (8.3 g). Experiments were performed at boiling temperature using a liquor/wood ratio equal to 5 g/g for 3 h. Subsequently they were cooled to room temperature.

The spent liquor obtained by filtration was concentrated through rotary vacuum evaporator at 60 °C, and approximately 100 mL concentrated sample was obtained, thereafter, 900 mL deionized water was added to precipitate the dissolved lignin. After 24 h, brown lignin was obtained by filtration.

Purification of AL

A mixture of dioxane and water with 9:1 volume ratio was employed to dissolve the lignin (about 15 mL solvent was used). Subsequently, centrifugal separation was performed to remove impurities.

Then lignin solution was added dropwise into 10-fold diethyl ether, centrifugal separation was performed again. Finally, the precipitate (lignin sample) was dried on P_2O_5 under vacuum condition for 5 days.

Preparation of lignin-containing polyurethane (LPU)

Acetic acid lignin (AL), TMP, and PEG with different molecular weights were dissolved in DMAc. MDI was added. The mixture was kept stirring in a water bath at 60 °C for 2 h. Then the temperature was increased to 70 °C. After 1.5 h, different dosages of APTS were added and the reaction was continued for another 0.5 h. The

Table 1 Composition of lignin-containing polyurethanes

Sample	Molecular weight of PEG	$n(NCO)/n(OH)$	Lignin/%[a]	APTS/%[b]	TMP/%[b]
PU	1,000	1.7:1	0	0	0
LPU1	1,000	1.7:1	43.3	0	0
LPU2	1,000	1.7:1	50.0	0	0
LPUP1	200	1.7:1	43.3	0	0
LPUP2	600	1.7:1	43.3	0	0
LPUP3	1,000	1.7:1	43.3	0	0
LPUP4	1,500	1.7:1	43.3	0	0
LPUP3-S1	1,000	1.7:1	43.3	1	0
LPUP3-S2	1,000	1.7:1	43.3	3	0
LPUP3-S3	1,000	1.7:1	43.3	4	0
LPUP3-S4	1,000	1.7:1	43.3	5	0
LPUP3-T1	1,000	1.7:1	43.3	0	1
LPUP3-T2	1,000	1.7:1	43.3	0	2
LPUP3-T3	1,000	1.7:1	43.3	0	3
LPUP3-T4	1,000	1.7:1	43.3	0	5
LPUP3-ST	1,000	1.7:1	43.3	2	1

[a] With respect to PEG

[b] With respect to total monomer mass

experimental conditions for preparing the LPU are given in Table 1. Lower NCO/OH ratio at 1.7:1 was employed in this research, since for LPU, the main shortcoming is its brittleness, and the flexibility of PU membranes can increase to some extent with the decrease of NCO/OH ratio.

Preparation of PU membranes

After the polymerization, the solution was immediately poured onto a PTFE plate, which was allowed to dry at room temperature for 2 days and then at 100 °C for 6 h. After de-molding, the film was submitted to vacuum drying over phosphorous pentoxide for 5 days.

Fourier transform infrared (FT-IR) analysis

Fourier transform infrared (FT-IR) spectra of all samples were recorded on a PerkinElmer Spectrum 100 FT-IR Spectrometer in the range of 4000–500 cm^{-1}.

Thermogravimetric (TG) analysis

The thermogravimetric (TG) experiments were performed in a TA Q500 Thermogravimetry (TG) analyzer. Membrane samples of about 10 mg was placed in a platinum sample pan and heated from 30 to 650 °C under N$_2$ or air at

a flow rate of 100 mL min^{-1}. In the case of the dynamic method, different heating profiles (5, 10, 20, and 40 °C min^{-1}) were investigated.

Kinetic analysis

In the degradation kinetics study, the corresponding kinetic parameters were determined based on the Friedman [36] and Flynn–Wall–Ozawa methods [37]. It was assumed that $d\alpha/dt$ has a linear relationship with k and $f(\alpha)$ in the adiabatic condition:

$$\frac{d\alpha}{dt} = kf(\alpha) \tag{1}$$

where $d\alpha/dt$ is the degradation rate, α is the conversion degree, k is the Arrhenius rate constant, $f(\alpha)$ is independent on temperature, but dependent on the degradation mechanism, which can be described by the following equation:

$$f(\alpha) = (1 - \alpha)^n \tag{2}$$

According to the Arrhenius equation, k can be described as follows:

$$k = A \exp\left(-\frac{E}{RT}\right) \tag{3}$$

where A is the preexponential factor, E is the activation energy, R is the universal gas constant, T is the temperature.

Equation 4 can be obtained when Eqs. 2 and 3 were substituted into Eq. 1

$$\frac{d\alpha}{dt} = A(1 - \alpha)^n \exp\left(-\frac{E}{RT}\right) \tag{4}$$

If assuming that a TG–DTG curve was measured at a constant heating rate, $\beta = dT/dt$, Eq. 4 could be rewritten as

$$\frac{d\alpha}{dT} = \frac{A}{\beta}(1 - \alpha)^n \exp\left(-\frac{E}{RT}\right) \tag{5}$$

Flynn–Wall–Ozawa Method

The Flynn–Wall–Ozawa method [37] is an integral method for determining the activation energies without any assumption on the reaction order.

Upon integration and the Doyle's approximation, Eq. 5 can be expressed as

$$\log F(\alpha) = \log A\frac{E}{R} - \log \beta - 2.315 - 0.4567\frac{E}{RT} \tag{6}$$

The activation energies, E, can be obtained from a plot of logarithms of heating rates, $\log \beta$, as a function of the reciprocal of temperature, T^{-1}.

Friedman method

The Friedman method is the most general technique used for determining the activation energy of degradation [36]. This method is independent of the heating rate, taking logarithm on both sides of Eq. 4

$$\ln\left(\frac{d\alpha}{dt}\right) = \ln A + n\ln(1-\alpha) - \frac{E}{RT} \qquad (7)$$

According to Eq. 7, $\ln A$ and $n\ln(1-\alpha)$ are constants if the conversion degree (α) is constant. And a plot of $\ln(d\alpha/dt)$ versus T^{-1} would result in a straight line with its slope equal to $-E/R$.

Results and discussion

Structure characterization

The structure of lignin, PU, and LPU1 was checked by FT-IR analysis. As shown in Fig. 1, several features indicated the occurrence of interaction between lignin and PU. (1) The reduction of the 3493 cm^{-1} free NH band in PU simultaneously with the appearance of wide band at 3309 cm^{-1} in LPU1 typical for bonded NH, which is merged with the 3443 cm^{-1} lignin –OH band; (2) The band of free –C=O at 1726 cm^{-1} in PU disappeared, while band of hydrogen-bonded –C=O at 1705 cm^{-1} was observed, which can be attributed to the formation of hydrogen bond between polar groups in lignin and urethane.

Effect of lignin

Figure 2 shows TG and DTG curves of AL, PU, and LPU. The decomposition temperatures at various mass loss percentages and the char residues are summarized in Table 2. It can be observed that lignin is decomposed in two stages, peaking at around 178.3 °C and 368.2 °C, respectively.
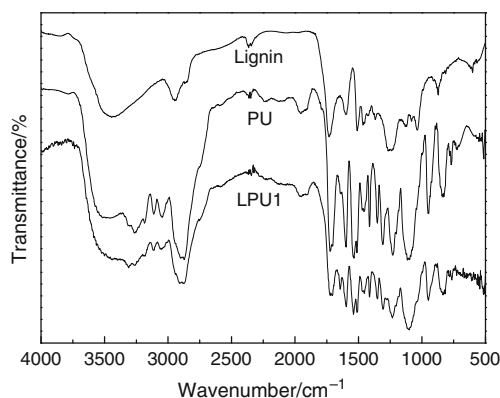
Fig. 1 FT-IR spectra of lignin, PU, and LPU1

The first stage (100.1–240.5 °C, peak at 178.3 °C) is related to the breaking of α- and β-aryl-alkyl-ether linkages, dehydration and decarboxylation reactions; while the second stage (245.2–470.4 °C, peak at 368.2 °C) is due to the cleavage of carbon–carbon linkages in the lignin structure [38].

It can be also observed that PU decomposes in three distinct stages. The first stage (242.5–364.7 °C, peak at 300.9 °C) can be ascribed to the breaking of urethane bonds. The second stage (364.3–460.6 °C, peak at 357.6 °C), which is rapid in the mass loss is due to PEG. The third stage (460.0–650.2 °C), is because of unzipping of the molecular chain [1, 39].

For the LPU, it was reported that the decomposition process of LPU films was similar to that of PU. LPU decomposes in two stages, peaking at around 290.0 and 350.0 °C, respectively. The first stage is related to breaking of the urethane group formed between isocyanate and phenolic hydroxyl groups of lignin, whereas the second stage is due to PEG [38–40]. While for the lignin-containing polyurethane (LPU1) in our research, the two stages became so close that one was a shoulder for the other, resulting in one main integral peak at 386.7 °C with a shoulder around 321.2 °C. These results indicate that the increase in the lignin concentration improved the LPU thermal stability. Such behavior could be explained by
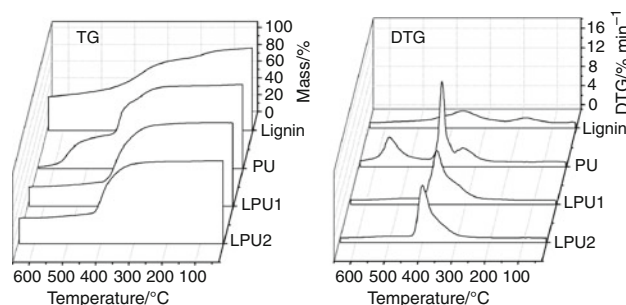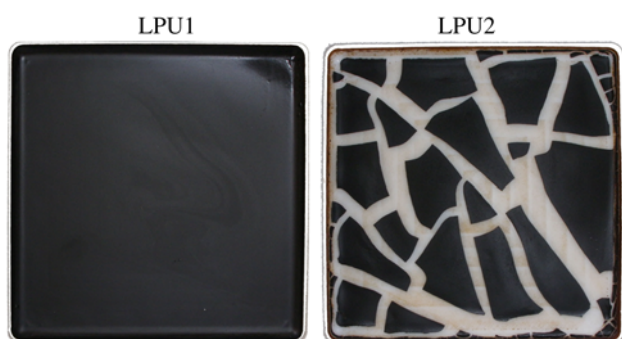

Fig. 2 TG and DTG curves of lignin, PU and LPU under nitrogen at 10 °C min^{-1}

Table 2 Results from TG, DTG analysis of lignin, PU, and LPU

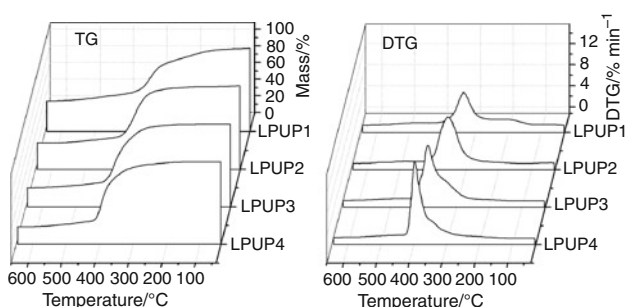| Sample ID	TG/°C				DTG	Residue/%
	$D_{0.1}$	$D_{0.2}$	$D_{0.3}$	$D_{0.5}$	T_{max}/°C	
Lignin	184.0	305.7	357.6	460.9	178.3, 368.2	40.39
PU	320.9	357.6	388.9	407.4	300.9, 357.6, 532.7	1.877
LPU1	309.2	339.7	361.0	386.3	386.7	22.88
LPU2	332.8	363.0	381.7	402.9	399.6	29.56

$D_{0.1}$ represents the degradation temperature at 10% mass loss. The number 0.1 represents mass loss, the others are the same

T_{max} is the temperature at the maximum rate of mass loss

Fig. 3 The surface morphology of LPU1 and LPU2 membrane

Fig. 4 TG and DTG curves of LPUP under nitrogen at 10 °C min^{-1}

Table 3 Results from TG, DTG analysis of LPUP

Sample ID	TG/°C				DTG	Residue/%
	$D_{0.1}$	$D_{0.2}$	$D_{0.3}$	$D_{0.5}$	T_{max}/°C	
LPUP1	221.5	296.3	325.8	367.6	201.5, 336.8	35.39
LPUP2	309.5	333.6	347.1	371.6	353.5	30.07
LPUP3	309.2	339.7	361.0	386.3	386.7	22.88
LPUP4	315.4	353.9	375.3	395.0	397.3	20.67

Fig. 5 TG and DTG curves of LPUP3-S under nitrogen at 10 °C min^{-1}

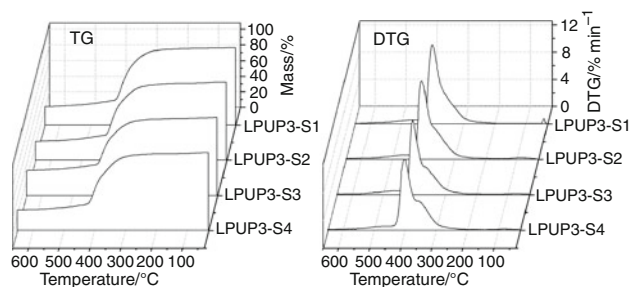taking into account the presence of high active chain reactions between MDI, PEG, and lignin.

Although the higher lignin concentration (50%) product (LPU2) exhibited higher thermal stability, the PU film formed is not in continuous phase, rupture took place as shown in Fig. 3. While continuous film can be formed when lignin concentration was 43.3%, which can be ascribed to the following two sides: on the one hand, lower NCO/OH ratio was adopted to decrease the stiffness of PU membrane; on the other hand, PEG with higher molecular weight was employed to improve the flexibility of PU membranes. Furthermore, it is also found that the char residue of LPU increases as lignin concentration increases.

Effect of PEG length

Figure 4 shows TG and DTG curves of LPU prepared by PEG of different molecular weights. The detailed decomposition temperatures at various mass loss percentages and the char residues are summarized in Table 3. It is evident that the length of soft segment (PEG) plays an important role, the degradation temperature at 10% mass loss increases from 221.5 to 315.4 °C when the number average molecular weight of PEG increases from 200 to 1,000, the same is true at higher mass losses, too. In addition, the temperature at which the maximum mass loss occurs is increased by 50 °C, indicating that a longer PEG is

beneficial for the thermal stability of the resulting polymer. The longer soft segment favors the phase separation and enhances the extent of inter-urethane hydrogen bonding [41].

Furthermore, the peak intensity decreases with the decrease in the PEG molecular weight, and extends to a lower temperature with a new broad shoulder appearing at 201.5 °C for LPUP1. The thermal degradation of LPUP4 occurs in a narrow temperature range compared with that with lower molecular weight soft segment. Thus, it can be concluded that LPUP with longer PEG has higher thermal stability due to the fact that its hard segment can be well protected by a longer PEG chain. Similar explanation was used to account for such phenomenon [42]. The stage mainly induced by PEG decomposition degrades faster due to its higher oxygen concentration.
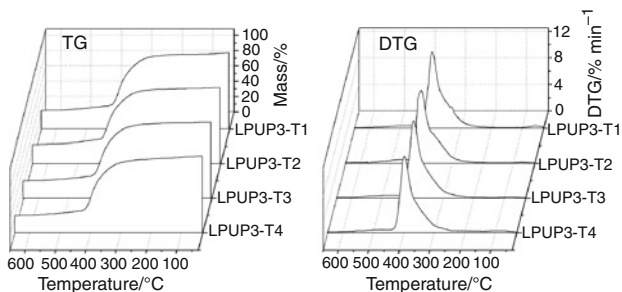
It is also found that the residue decreased from 35.39% to 20.67% with the increase in the PEG molecular weight (as shown in Table 3). This is because the oxygen concentration (based on total monomer mass) is increased with the increase in the PEG molecular weight.

Effect of cross-linking agent

The influence of cross-linking agent (APTS and TMP) on the thermal stability of LPU was also studied based on the TG and DTG analyses, as shown in Figs. 5 and 6. The results are summarized in Table 4. It can be found that the degradation temperatures increase with the addition of

APTS, suggesting that APTS can improve the thermal stability of the resulting polymer, which can be ascribed to the increased cross-linking degree. On the other hand, it was reported that the thermal stability is largely determined by the strength of the covalent bonds between the atoms

forming the polymer molecules. The C–C bond energy is less than that of C-Si and Si-O bonds [43]. With the increase in APTS concentration, the rudimental networks formed by APTS increase, resulting in higher degradation temperature, too.

However, a slight decrease in the degradation temperature occurs when the ATPS charge exceeds 4%, and the lower side decomposition peaks in the temperature range from 350.1 to 359.5 °C become wider with increasing APTS concentration. It has been reported that the increased cross-linking degree can induce two opposite effects on the properties of PU [29, 30]. On one hand, it will decrease the size and number of hard-segment domain, resulting in microphase mixing, thus the formation of a more homogeneous network, this would increase the thermal stability. On the other hand, it can destroy the regularity of the hard segment, resulting in less optimum stacking of chain segments, thus a lower thermal stability.
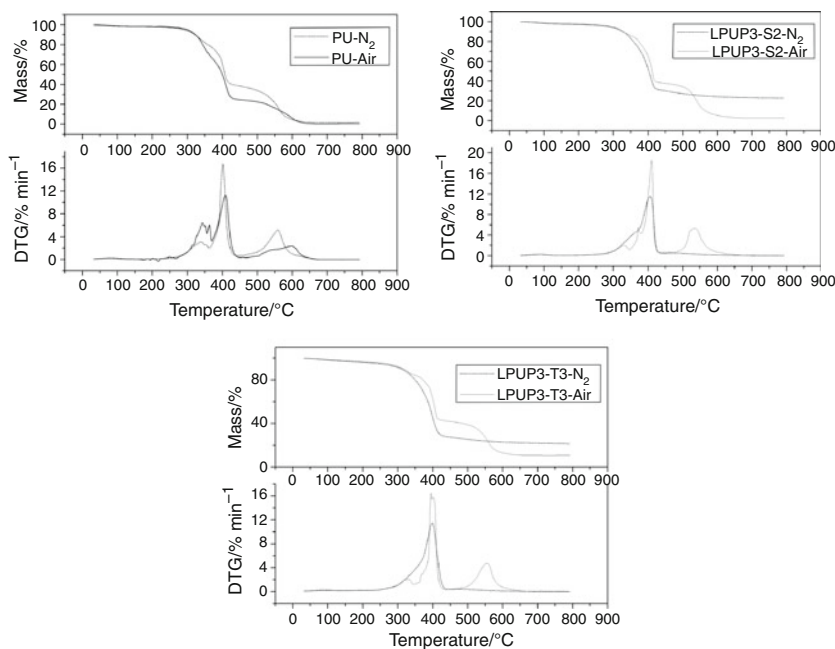
A similar phenomenon was also observed for the lignin-based polyurethane samples with TMP addition, as shown in Fig. 5. It is evident that the degradation temperature increased to 323.7 °C with a 2% TMP addition, but decreased to 310.9 °C at a 5% TMP addition.

Furthermore, the results in Table 4 indicated that APTS, as a cross-linking agent, is more effective in increasing the thermal stability of the PU films than TMP.

### Stability under thermo-oxidative conditions

For a better understanding of the oxidation process of the PU produced, TG and DTG curves of PU, LPUP3-S2, and LPUP3-T3 under nitrogen and air were compared.

Fig. 6 TG and DTG curves of LPUP3-T under nitrogen at 10 °C min^{-1}

Table 4 Results from TG, DTG data of LPUP3-S and LPUP3-T

Sample ID	TG/°C				DTG	Residue/%
	$D_{0.1}$	$D_{0.2}$	$D_{0.3}$	$D_{0.5}$	T_{max}/°C	
LPUP3	309.2	339.7	361.0	386.3	386.7	22.88
LPUP3-S1	327.8	358.7	378.0	399.8	400.4	22.74
LPUP3-S2	328.1	358.1	378.7	402.0	404.9	22.86
LPUP3-S3	330.9	362.2	384.3	407.2	405.7	30.65
LPUP3-S4	325.4	354.3	376.3	402.1	402.5	24.90
LPUP3-T1	318.8	350.6	371.2	394.0	393.6	23.05
LPUP3-T2	323.7	356.4	378.0	401.7	402.6	23.65
LPUP3-T3	319.1	352.3	372.6	395.6	396.6	21.89
LPUP3-T4	310.9	349.7	371.6	395.7	398.1	21.36

Fig. 7 TG and DTG curves of PU, LPUP3-S2, and LPUP3-T3 under nitrogen and air at 10 °C min^{-1}

Table 5 Results from TG, DTG data of PU, LPUP3-S2 and LPUP3-T3

Sample ID	TG/°C				DTG	Residue/%
	$D_{0.1}$	$D_{0.2}$	$D_{0.3}$	$D_{0.5}$	T_{max}/°C	
PU-N$_2$	320.9	357.6	388.9	407.4	300.9, 357.6, 532.7	1.877
PU-Air	323.3	343.8	362.3	399.7	341.9, 362.4, 409.8, 598.9	0.480
LPUP3-S2-N$_2$	328.1	358.1	378.7	402.0	356.5, 404.9	22.86
LPUP3-S2-Air	324.9	371.8	392.5	410.9	329.6, 370.7, 409.8, 533.1	2.568
LPUP3-T3-N$_2$	319.1	352.3	372.6	395.6	396.6	21.89
LPUP3-T3-Air	322.5	370.7	389.7	406.7	329.6, 403.7, 570.1	1.365
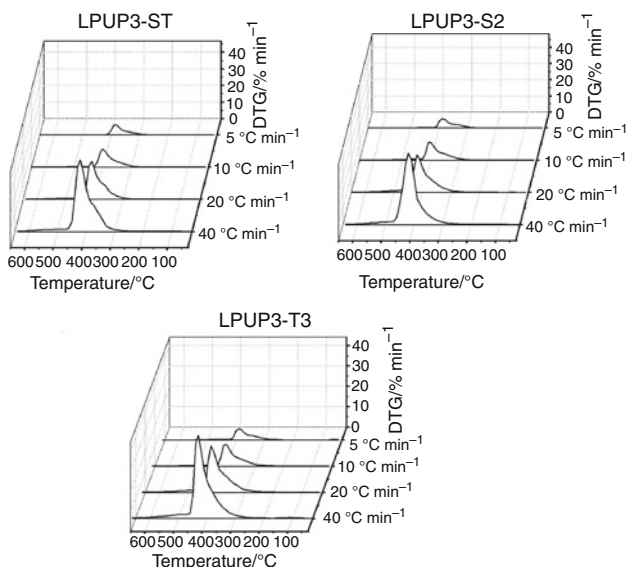
Fig. 8 Dynamic DTG curves of LPUP3-ST, LPUP3-S2, and LPUP3-T3 at different heating rates
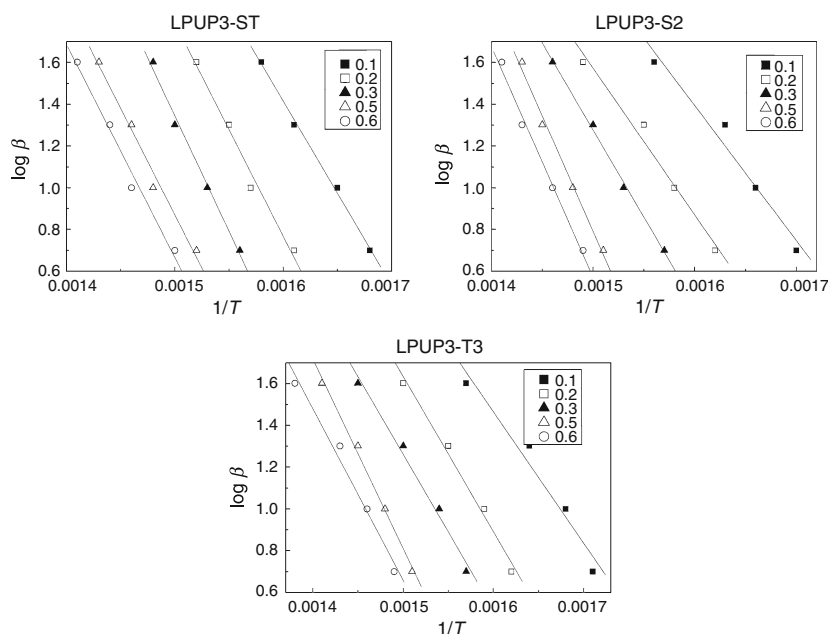
Figure 7 shows the TG and DTG curves of PU, LPUP3-S2, and LPUP3-T3 under air and nitrogen, and the summary results are given in Table 5. It is evident that DTG curves obtained in air exhibit multistage process, which is related to the oxidation reactions of the respective soft and hard segments. The first degradation stage can be attributed to the initial oxidative attack on the α-carbon atom to the oxygen, resulting in chain scission [29, 44]. The oxidation reactions of the hard segment occur in a later stage than those of soft segment [45]. It is also possible that the last step during the degradation in air (in the temperature range between 500 and 600 °C) is due to the decomposition of the char formed in the earlier steps [46, 47].

The samples heated under air show negligible residues while those under nitrogen have more residues. These results can be explained by less chain scissions during the course of heating under nitrogen.

In addition, the degradation temperatures at 10% mass loss for PU in nitrogen are slightly lower than those degraded in air, and an increase in the stability of PU is

Fig. 9 Flynn–Wall–Ozawa plots of LPUP3-ST, LPUP3-S2, and LPUP3-T3 at different conversions

observed under nitrogen from 325 °C. However, with respect to PU modified by lignin, the opposite trend was observed. In the approximate range from 300 to 550 °C, LPUP3-S2 and LPUP3-T3 heated under air show less mass losses than those heated under nitrogen. This was perhaps due to the predominant crosslinking reactions, as compared with the chain scission reactions [39, 48]. These results also indicate that the oxidative degradation is decreased due to the addition of lignin.

Kinetic analysis

Dynamic differential thermogravimetry (DTG) curves for the LPUP3-TS, LPUP3-S2, and LPUP3-T3 samples under nitrogen at various heating rates of 5, 10, 20, 40 °C min^{-1} are shown in Fig. 8. Their corresponding Flynn–Wall–Ozawa plots of ln(dα/dt) versus 1/T for constant values of conversion are shown in Fig. 9. The results on their activation energy (E_a) and correlation coefficient (R) obtained from the Flynn–Wall–Ozawa method are presented in Table 6. Figure 10 displays the Friedman plots of LPUP3-TS, LPUP3-S2, and LPUP3-T3 at different conversions, with the results summarized in Table 7.

A good linear relationship is established for the Flynn–Wall–Ozawa plots of the three samples versus 1/T. Therefore, the degradation reaction of lignin-based PU is a first order reaction.

On summarizing the data obtained from the Flynn–Wall–Ozawa method and the Friedman method, it can be found that the correlation coefficients of the first method are all greater than 0.98, demonstrating that the Flynn–Wall–Ozawa method is applicable to the present system.

Table 6 Activation energies calculated using the Flynn–Wall–Ozawa method

Sample ID	Conversion (α)				
	0.1	0.2	0.3	0.5	0.6
LPUP3-ST					
E_a/KJ mol^{-1}	160.6	185.8	195.5	197.8	196.6
R	0.9983	0.9970	0.9954	0.9911	0.9823
LPUP3-S2					
E_a/KJ mol^{-1}	124.4	130.0	151.0	189.8	186.4
R	0.9883	0.9942	0.9982	0.9962	0.9997
LPUP3-T3					
E_a/KJ mol^{-1}	118.8	130.0	145.2	159.6	143.2
R	0.9902	0.9908	0.9933	0.9960	0.9853

Table 7 Activation energies calculated using the Friedman method

Sample ID	Conversion (α)				
	0.1	0.2	0.3	0.5	0.6
LPUP3-ST					
E_a/KJ mol^{-1}	179.5	197.8	205.4	196.2	202.5
R	0.9955	0.9960	0.9925	0.9805	0.9275
LPUP3-S2					
E_a/KJ mol^{-1}	120.0	159.1	201.4	191.4	189.2
R	0.9966	0.9997	0.9946	0.9986	0.9946
LPUP3-T3					
E_a/KJ mol^{-1}	121.6	143.6	155.4	165.8	171.5
R	0.9809	0.9950	0.9972	0.9950	0.9936

Fig. 10 Friedman plots of LPUP3-ST, LPUP3-S2, and LPUP3-T3 at different conversions
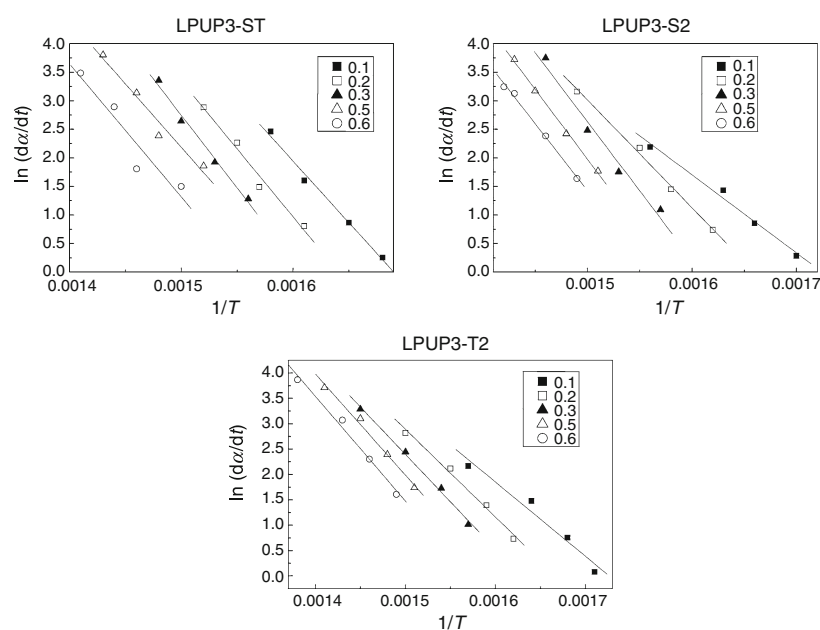
For the Friedman method, the correlation coefficient for LPUP3-ST at 60% mass is 0.932, while others were greater than 0.98.

It can be also found that the LPU samples modified with APTS exhibited higher activation energies than those modified with TMP. Furthermore, the maximum activation energy was found for the sample modified with both APTS and TMP.

Conclusions

The degradation behaviors of PU and LPU were investigated. FT-IR certified the occurrence of interaction between lignin and PU. The degradation temperature increased with the increase in the amount of lignin added, and PU membranes of continuous phase can be formed when lignin concentration was 43.3%, but rupture took place at a 50% lignin concentration. The addition of PEG increased the thermal stability of LPUP. The higher the PEG molecular weight, the higher the PU stability; the degradation temperature at 10% mass loss increased from 221.5 °C to 315.4 °C with the PEG molecular weight increased from 200 to 1,000. The addition of cross-linking agents, APTS, and TMP to the preparation of PU also increased the thermal stability of the resulting products, and the maximum stability was found at 4% APTS and 2% TMP, respectively. A further increase of these cross-linking agents resulted in a slight decrease in the thermal stability. Furthermore, LPU exhibited multistage degradation process under air and displayed higher thermal stability than those heated under nitrogen in the temperature range of 300–550 °C. The kinetic analyses demonstrated that the Flynn–Wall–Ozawa method can be applied to the LPU system with a good correlation coefficient. The results also showed that the LPU samples modified with APTS exhibited higher activation energy than those modified with TMP. The maximum activation energy was found for the sample modified with the simultaneous addition of APTS and TMP.

References

1. Zhang LN, Huang J. Effects of nitrolignin on mechanical properties of polyurethane—nitrolignin films. J Appl Polym Sci. 2001;80:1213–9.
2. Lora JH, Glasser WG. Recent industrial applications of lignin: a sustainable alternative to nonrenewable materials. J Polym Environ. 2002;10:39–48.
3. Hatakeyama T, Izuta Y, Hirose S, Hatakeyama H. Phase transitions of lignin-based polycaprolactones and their polyurethane derivatives. Polymer. 2002;43:1177–82.
4. Hatakeyama H, Hatakeyama T. Environmentally compatible hybrid-type polyurethane foams containing saccharide and lignin components. Macromol Symp. 2005;224:219–26.
5. Nadji H, Bruzzèse C, Belgacem MN, Benaboura A, Gandini A. Oxypropylation of lignins and preparation of rigid polyurethane foams from the ensuing polyols. Macromol Mater Eng. 2005; 290:1009–16.
6. Akhtar T, Lutfullah G, Nazli R. Synthesis of lignin based phenolic resin and its utilization in the exterior grade plywood. J Chem Soc Pak. 2009;31:304–8.
7. Ibrahim MNM, Ghani AMd, Zakaria N, Shuib S, Sipaut CS. Formulation of an environmentally friendly adhesive for wood. Macromol Symp. 2008;274:37–42.
8. Bonini C, D'Auria M, Emanuele L, Ferri R, Pucciariello R, Sabia AR. Polyurethanes and polyesters from lignin. J Appl Polym Sci. 2005;98:1451–6.
9. Michinobu T, Hishida M, Sato M, Katayama Y, Masai E, Nakamura M, et al. Polyesters of 2-pyrone-4,6-dicarboxylic acid (PDC) obtained from a metabolic intermediate lignin. Polym J. 2008;40:68–75.
10. Kubo S, Kadla JF. Poly(ethylene oxide)/organosolv lignin blends: relationship between thermal properties, chemical structure, and blend behavior. Macromolecules. 2004;37:6904–11.
11. Cazacu G, Mihaies M, Pascu MC, Profire L, Kowarskik AL, Vasile C. Polyolefin/lignosulfonate blends, 9 functionalized polyolefin/lignin blends. Macromol Mater Eng. 2004;289:880–9.
12. Cazacu G, Pascu MC, Profile L, Kowarski AI, Mihaes M, Vasile C. Lignin role in a complex polyolefin blend. Ind Crop Prod. 2004;20:261–73.
13. Li Y, Sarkanen S. Alkylated kraft lignin-based thermoplastic blends with aliphatic polyesters. Macromolecules. 2002;35:9707–15.
14. Wu RL, Wang XL, Li F, Li HZ, Wang YZ. Green composite films prepared from cellulose, starch and lignin in room-temperature ionic liquid. Bioresour Technol. 2009;100:2569–74.
15. Wei M, Fan L, Huang J, Ai FJ, Fan LH, Zheng H. Role of star-like hydroxylpropyl lignin on properties of soy protein plastics. Macromol Mater Eng. 2006;291:524–30.
16. Jahan MS, Chowdhury DAN, Islam MK. Atmospheric formic acid pulping and TCF bleaching of dhaincha (*Sesbania aculeate*), kash (*Saccharum spontaneum*) and banana stem (*Musa cavendish*). Ind Crop Prod. 2007;26:324–31.
17. Ligero P, Villaverde JJ, de Vega A, Bao M. Delignification of eucalyptus globulus saplings in two organosolv systems (formic and acetic acid) preliminary analysis of dissolved lignins. Ind Crop Prod. 2008;27:110–7.
18. Thring RW, Chornet E, Overend RP. Fractionation of woodmeal by prehydrolysis and thermal organosolv. Process strategy, recovery of constituents, and solvent fractionation of lignins so produced. Can J Chem Eng. 1993;71:116–23.
19. Pye EK, Lora JH. The Alcell process: an alternative to kraft pulping. Tappi J. 1991;74:113–7.
20. Ni Y, Van Heiningen ARP, Lora J, Magdzinski L, Pye EK. A novel ozone bleaching technology for the ALCELL process. J Wood Chem Technol. 1996;16:367–80.
21. Ni Y, Hu Q. Alcell lignin solubility in ethanol-water mixtures. J Appl Polym Sci. 1995;57:1441–6.
22. Pan X, Sano Y. Fractionation of wheat straw by atmospheric acetic acid process. Bioresour Technol. 2005;96:1256–63.
23. Poppius L, Mustonen KR, Huovila T, Sundquist J. MILOX pulping with acetic acid/peroxyacetic acid. Paperi ja Puu. 1991;73:154–8.
24. Jahan MS. Studies on the effect of prehydrolysis and amine in cooking liquor on producing dissolving pulp from jute (*Corchorus capsularis*). Wood Sci Technol. 2009;43:213–24.

25. Vanderlaan MN, Thring RW. Polyurethanes from Alcell lignin fractions obtained by sequential solvent extraction. Biomass Bioenerg. 1998;14:525–31.

26. Reimann A, Mörck R, Yoshida H, Hatakeyama H, Kringstad KP. Kraft lignin in polyurethanes III. Effects of the molecular weight of PEG on the properties of polyurethanes from a kraft lignin-PEG-MDI system. J Appl Polym Sci. 1990;41:39–50.

27. Reimann A, Mörck H, Hatakeyama H, Kringstad KP. Effects of the structure of lignin on the properties of lignin-based polyurethanes. Sixth international symposium on wood and pulping chemistry; 1991, p. 523.

28. Rials TG, Glasser WG. Engineering plastics from lignin. 5. Effect of crosslink density on polyurethane film properties-variation in polyol hydroxyl content. Holzforschung. 1984;38:263–9.

29. Fan QC, Xiao CB. Effects of crosslinking density on structure and properties of interpenetrating polymer networks from polyurethane and nitroguar gum. Polym Compos. 2008;29:758–67.

30. Chiou BS, Schoen PE. Effect of crosslinking on thermal and mechanical properties of polyurethanes. J Appl Polym Sci. 2002;83:212–23.

31. Li XR, Fei GQ, Wang HH. Mechanical and surface properties of membranes prepared from waterborne cationic hydroxyl-terminated polydimethylsiloxane/polyurethane surfactant-free microemulsion. J Appl Polym Sci. 2006;100:40–6.

32. Chen S, Sui J, Chen L, Pojman JA. Polyurethane-nanosilica hybrid nanocomposites synthesized by frontal polymerization. J Polym Sci. 2005;43:1670–80.

33. Chen S, Sui J, Chen L. Positional assembly of hybrid polyurethane nanocomposites via incorporation of inorganic building blocks into organic polymer. Colloid Polym Sci. 2004;283:66–73.

34. Agić A, Bajsić EG. Strategy for kinetic parameter estimation-thermal degradation of polyurethane elastomers. J Appl Polym Sci. 2007;103:764–72.

35. Hatakeyama H, Kosugi R, Hatakeyama T. Thermal properties of lignin- and molasses-based polyurethane foams. J Therm Anal Calorim. 2008;92:419–24.

36. Joshi P, Madras G. Degradation of polycaprolactone in supercritical fluids. Polym Degrad Stabil. 2008;93:1901–8.

37. Barral L, Cano J, Lpez J, López-Bueno I, Nogueira P, Abad MJ, Ramírez C. Decomposition behavior of epoxy-resin systems cured by diamines. Eur Polym J. 2000;36:1231–40.

38. Ciobanu C, Ungureanu M, Ignat L, Ungureanu D, Popa VI. Properties of lignin-polyurethane films prepared by casting method. Ind Crop Prod. 2004;20:231–41.

39. Hirose S, Kobashigawa K, Izuta Y, Hatakeyama H. Thermal degradation of polyurethanes containing lignin studied by TG-FTIR. Polym Int. 1998;47:247–56.

40. Hatakeyama H, Nakayachi A, Hatakeyama T. Thermal and mechanical properties of polyurethane-based geocomposites derived from lignin and molasses. Composites A. 2005;36:698–704.

41. Wang TL, Hsieh TH. Effect of polyol structure and molecular weight on the thermal stability of segmented poly (urethaneureas). Polym Degrad Stabil. 1997;55:95–102.

42. Wang HH, Shen YD, Fei GQ, Li XR, Liang Y. Micromorphology and phase behavior of cationic polyurethane segmented copolymer modified with hydroxysilane. J Colloid Interface Sci. 2008;324:36–41.

43. Guo TY, Chen X, Song MD, Zhang BH. Preparation and properties of Core [poly(styrene-n-butyl acrylate)]-shell [poly (styrene-methyl methacrylate-vinyl triethoxide silane)] structured latex particles with self-crosslinking characteristics. J Appl Polym Sci. 2006;100:1824–30.

44. Xiao HX, Yang S, Kresta JE, Frisch KC, Higley DP. Thermostability of urethane elastomers based on p-phenylene diisocyanate. J Elastomers Plast. 1994;26:237.

45. Ferguson J, Petrovic Z. Thermal stability of segmented polyurethanes. Eur Polym J. 1976;12:177–81.

46. Herrera M, Matuschek G, Kettrup A. Main products and kinetics of the thermal degradation polyamides. Chemosphere. 2001;42:601–7.

47. Herrera M, Matuschek G, Kettrup A. Thermal degradation of thermoplastic polyurethane elastomers (TPU) based on MDI. Polym Degrad Stabil. 2002;78:323–31.

48. Shieh YT, Chen HT, Liu KH, Twu YK. Thermal degradation of MDI-based segmented polyurethanes. J Polym Sci. 1999;37:4126–34.